AIP Journal of Applied Physics

Classical interatomic potential model for Si/H/Br systems and its application to atomistic Si etching simulation by HBr +

T. Nagaoka, K. Eriguchi, K. Ono, and H. Ohta

Citation: Journal of Applied Physics **105**, 023302 (2009); doi: 10.1063/1.3056391
View online: http://dx.doi.org/10.1063/1.3056391
View Table of Contents: http://scitation.aip.org/content/aip/journal/jap/105/2?ver=pdfcov
Published by the AIP Publishing

Classical interatomic potential model for Si/H/Br systems and its application to atomistic Si etching simulation by HBr^+

T. Nagaoka,[a] K. Eriguchi, K. Ono, and H. Ohta[b]
Department of Aeronautics and Astronautics, Graduate School of Engineering, Kyoto University, Yoshida-Honmachi, Sakyo-ku, Kyoto 606-8501, Japan

(Received 29 September 2008; accepted 18 November 2008; published online 21 January 2009)

An interatomic potential model for Si/H/Br systems has been developed for performing classical molecular dynamics simulations of Si etching processes by HBr plasmas. The potential form used here is the improved Stillinger–Weber potential function involving a correction term in order to predict the reaction dynamics more accurately. Parameters were determined based on *ab initio* data obtained from previous works on Si/Br systems by [Ohta *et al.* J. Appl. Phys. **104**, 073302 (2008)]. By using this model, we performed Si etching simulations by monoenergetic HBr^+ and Br^+ beams. H atom has about 1% of the translational energy of cluster ions due to the small H/Br mass ratio (=1.0/79.9); therefore, H atoms in HBr^+ behave like H radicals. This results in higher etch yields by HBr^+ than those by Br^+ in the low-energy region (less than 100 eV). This can be attributed to the chemical enhancement induced by the formation of Si–H bonds. On the other hand, yields by HBr^+ and Br^+ were almost the same in the high-energy region (more than 100 eV), where physical sputtering was relatively dominant and the contribution of H was small. © *2009 American Institute of Physics*. [DOI: 10.1063/1.3056391]

I. INTRODUCTION

The interaction between chemical plasmas and the semiconductor surface is a key topic in plasma processing technologies, where 10 nm scale processing can be achieved.[1] In this research field, atomic-scale numerical simulations for reaction processes during plasma etching attracted much attention.[2] During plasma processing, high-energy ions (typically 10–500 eV) accelerated in the plasma sheath are injected into the material surface.[3,4] In such cases, a very large number of simulation particles are required for dynamically tracking the reactions. Therefore, a classical molecular dynamics (MD) simulation using a preconstructed interatomic potential model might be unique because the low simulation cost incurred facilitates a systematic parameter survey, e.g., as a function of beam energies and angles.[2,5] The simulation for more realistic plasma etching conditions including radicals incurs considerably larger costs than those encountered in beam etching simulations.[5]

The construction of a potential model is vital for performing classical MD simulations. Here, we briefly summarize the Stillinger–Weber (SW) potential models developed for plasma etching simulations. Originally, Stillinger and Weber[6] developed a potential model with two-body and three-body functions for Si and F systems. Feil *et al.*[7] applied this functional form to Si and Cl systems by determining new parameter sets. Ohta and Hamaguchi[8] developed two sets of potential models for Si–O–F and Si–O–Cl systems based on previously reported potential models for Si–F, Si–Cl, and Si–O systems with additional *ab initio* data. Potential models for Si–O–C–F systems for performing the MD simulations of SiO_2 etching by fluorocarbon plasmas were reported by Smirnov *et al.*[9] After that, Smirnov *et al.*[10] further extended the SW models to Si–O–C–H systems for plasma etching simulations with low-*k* dielectric materials. Most recently, Ohta *et al.*[11] determined the parameter set for Si/Br systems completely based on the *ab initio* data.

On the other hand, the potential form itself has been re-examined. Recently, Iwakawa *et al.*[12] clarified how the penetration energy of ions into lattices affects the reaction dynamics and structures of surface reaction layers. They concluded that the penetration energy has a profound effect on the prediction of the surface structure. Furthermore, Ohta *et al.*[13] found that the original SW model has a flaw in the three-body function, which is an overestimation of the repulsive force caused by the simple summation of the three-body functions, where a halogen atom is surrounded by more than three atoms. This situation definitely occurs when a high-energy halogen is impinged on a Si lattice. To prevent this, an improved potential form with a correction term in the three-body function has been proposed.

Generally, halogens show strong chemical reactivity in the Si etching processes. Since the etching processes reduced to the deep submicron scale, HBr plasmas have been introduced in actual manufacturing processes. There are published reports on fundamental experiments to this end.[14,15] Vitale *et al.*[15] revealed the ion flux composition of HBr plasmas. In their case, the ion flux composition was Br^+ (43%), HBr^+ (42%), and Br_2^+ (15%) (see Table III in Ref. 15). In addition, various radicals (HBr, Br, Br_2, and H) were also

[a]Electronic mail: naga2118@yahoo.co.jp.
[b]Present address: Materials Department, University of California, Santa Barbara, CA 93106, U.S.A. Electronic mail: hiroaki.ohta.aug18@gmail.com.

present in low-temperature HBr plasmas, where the reported value of the neutral-to-ion-flux ratio was 2200–22 000. Therefore, in actual plasma experiments, we cannot identify the individual role of each ion. Although beam experiments are now possible, they are sometimes prohibitively expensive. Hence, ideal simulations to study them are imperative.

In this study, we present a parameter set for Si/H/Br systems to realize atomistic simulations of state-of-the-art Si etching processes by HBr-containing plasmas. As a potential form, we use improved SW-type potential with a correction term. The simulation results of Si etching by HBr^+ and Br^+ beams using the new potential model are reported.

II. INTERATOMIC POTENTIAL MODEL FOR SI/H/BR SYSTEMS

Let us introduce our potential model.[6,8,11,13] We consider the atomic interactions only among charge-neutral species and the adiabatic assumption for electron dynamics for the system. The total energy of the atomic system is expressed by the summation of the two- and three-body potentials with a parameter ε as

$$\Phi = \sum_{i<j} v_{ij}(r_{ij}) + \sum_{i,j,k} \varepsilon_i h_{jik}(r_{ij}, r_{ik}, \theta_{jik}), \tag{1}$$

where $r_{ij}=|\mathbf{r}_i-\mathbf{r}_j|$ denotes the distance between the ith and jth atoms located at $\mathbf{r}_i$ and $\mathbf{r}_j$, respectively. θ_{jik} is the angle spanned by $\mathbf{r}_j-\mathbf{r}_i$ and $\mathbf{r}_k-\mathbf{r}_i$. Further, ε_i is a correction term to prevent unintended overestimation of repulsive interactions by the three-body function.[13] For $\varepsilon_i=1$, Eq. (1) is identical to the original SW model.[4,5] The two-body function is given by

$$v_{ij}(r_{ij}) = A_{ij}(B_{ij}r_{ij}^{-p_{ij}} - 1)\exp[C_{ij}/(r_{ij}-a_{ij})]. \tag{2}$$

This expression describes the repulsive and attractive interactions among two atoms. The parameters A_{ij}, B_{ij}, C_{ij}, p_{ij}, and a_{ij} depend on the element type of the ith and jth elements. The three-body function $h_{jik}(r_{ij}, r_{ik}, \theta_{jik})$ is given by

$$h_{jik}(r,s,\theta) = \lambda_{jik} \exp[\gamma_{jik}^j/(r-a_{jik}^j) + \gamma_{jik}^k/(s-a_{jik}^k)] \tag{3}$$

for $i \in$ halogen (=F, Cl, Br, H, etc.) or by

$$h_{jik}(r,s,\theta) = \lambda_{jik} \exp[\gamma_{jik}^j/(r-a_{jik}^j) + \gamma_{jik}^k/(s-a_{jik}^k)] \times |\cos\theta - \cos\theta_{jik}^0|^{2\alpha_{jik}} \tag{4}$$

for $i \in$ Si. Equation (3) is used to cancel the additional attractive interactions resulting from the simple summation of v_{ij}. On the other hand, Eq. (4) is used to restrict the angles between two covalent bonds. λ_{jik}, γ_{jik}^j, γ_{jik}^k, a_{jik}^j, a_{jik}^k, θ_{jik}^0, a_{jik}^j, and a_{jik}^k denote the parameters that depend on the species of the (i,j,k) triplet. Previous studies have shown that these functions could reconstruct the *ab initio* data with high accuracy when the systems included only two or three atoms.[8,11]

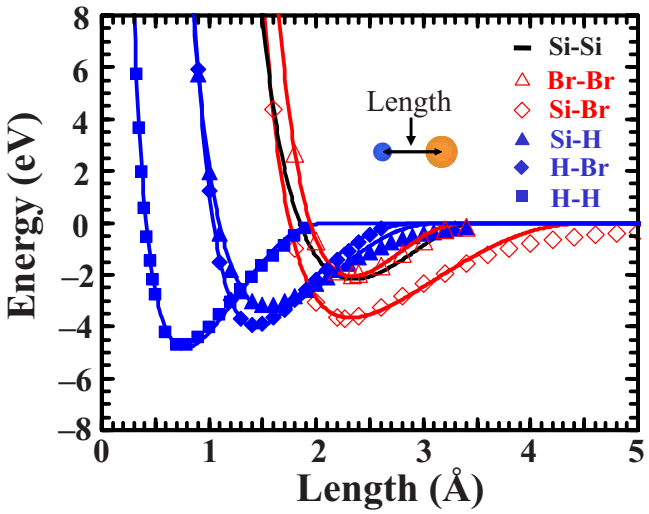

FIG. 1. (Color online) Potential energy curves (lines) and *ab initio* data (points) for two-body interactions. The zero reference is the sum of the potential energies of isolated atoms.

A parameter for three-body function ε_i, which is a function of the positions of neighboring atoms, is given by

$$\varepsilon_i = \varepsilon_i(m_i)\begin{cases} =1 & m_i \le 2, \\ =h(m_i)\dfrac{2}{m_i} + [1-h(m_i)]\cdot 1 & 2 < m_i < 3, \\ =\dfrac{2}{m_i} & 3 \le m_i, \end{cases} \tag{5}$$

for $i \in$ halogen. $\varepsilon_i=1$ for $i \notin$ halogen. $m_i(=\Sigma_j b_{ij})$ is the bonding number of the ith atom. Here, $h(x) = \{1+\exp[-a(x-b)]\}^{-1}$ is a smoothing function, where we use $a=10$ and $b=2.5$. The degree of bond formation b_{ij} is evaluated as $b_{ij}=v_{ij}/v_{ij(\min)}$ for $r_{ij}>r_{ij(\min)}$. Here, $v_{ij(\min)}$ is the minimum of v_{ij} at $r_{ij}=r_{ij(\min)}$. For $r_{ij}<r_{ij(\min)}$, $b_{ij}=1$. The detailed derivation is published elsewhere.[13] This parameter prevents the overestimation of the penetration energy of ions into the lattice, which is a key factor to predict the surface reaction dynamics.[12,13] Note that Hanson *et al.*[16] proposed the SW model with bond-order correction to improve Si–Si and Si–Cl bond strengths. They improved the accuracy of attractive interactions while our model improved the repulsive interactions.

All parameters have been determined based on the *ab initio* data obtained from quantum chemical calculations using GAUSSIAN03.[17] The procedure was completely the same as that in the previous work on Si/Br systems.[11] It should be noted that a parameter ε was not taken into account when we determined the parameters because the *ab initio* data used here were those for clusters including two or three atoms. The *ab initio* data and the obtained potential curves are shown in Figs. 1–3. The globally optimized parameter set for

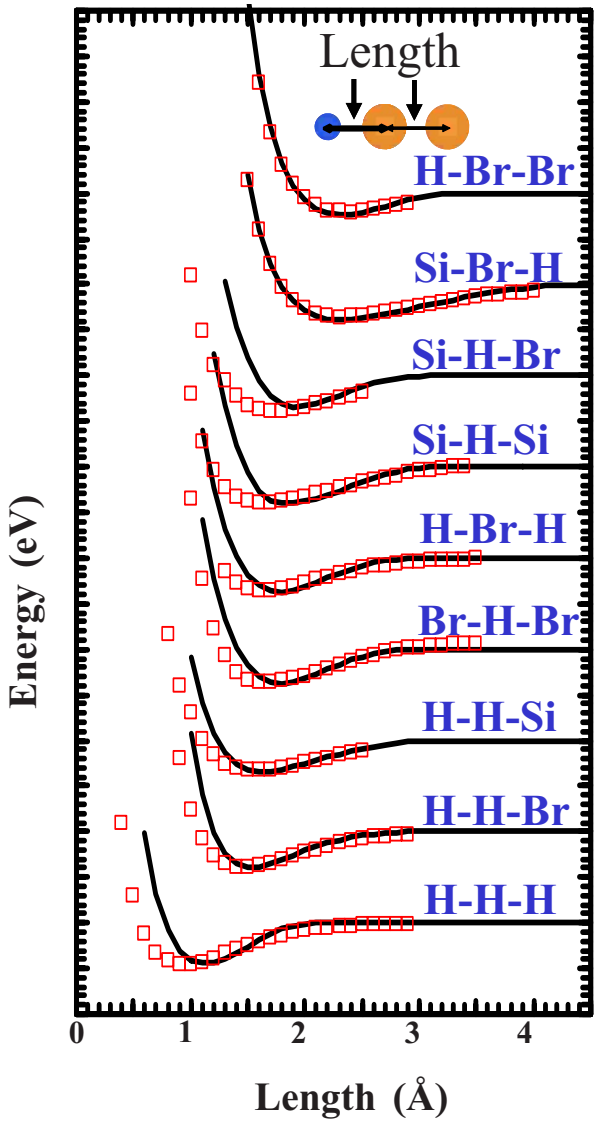

FIG. 2. (Color online) Potential energy curves (lines) and *ab initio* data (points) for *X*-Br-*X* or *X*-H-*X* (*X*=H, Br, Si) configurations in alignment as a function of both the bond lengths, where two bond lengths were changed simultaneously. The zero references for each configuration are the sum of the potential energies of isolated atoms. Here, each case is plotted with shift.

Si/H/Br systems is shown in Table I. The calculated bond energy (potential minimums) and bond lengths for the pair atoms are summarized in Table II. Although the potential curves for *X*-Br-*X* or *X*-H-*X* (*X*=Si, H, and Br) configurations were slightly different from the *ab initio* data at short distances, the depths of the potential minimums obtained using our model were almost the same as the *ab initio* data.

III. SI ETCHING SIMULATION BY HBR+

MD simulations of Si etching by high-energy HBr^+ or Br^+ bombardment were performed by using our potential model. Our simulation technique is completely the same as that proposed in earlier works.[2,8,11–13] The target atoms are initially located in the structure of the diamond lattice, where the top surface corresponds to (100). The square-shaped

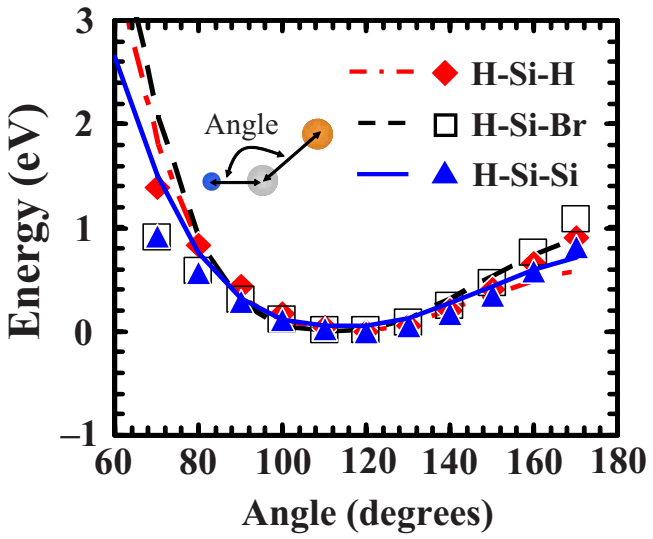

FIG. 3. (Color online) Potential energy curves (lines) and *ab initio* data (points) for *X*-Si-*X* (*X*=H, Br, Si) configuration. The zero references were the energies at optimized configurations for each case.

Si(100) surface has a side length of 32.58 Å (area: 1061 $Å^2$) and a monolayer that initially contains 72 Si atoms. Atoms in the bottom layer are fixed during the simulation and periodical boundaries are imposed along the horizontal direction. The initial target temperature before ion bombardment is 300 K.

To this Si(100) surface, ions with an energy of 10–500 eV are repeatedly injected from randomly selected horizontal locations. It is sometimes more convenient to measure the dose of the impinging particles in monolayer units, where 1 ML corresponds to 72 impinging particles. After the injection of each atom, we allow the system to evolve for 0.7 ps under a constant total energy. For the time integral, the actual mass numbers of ^1H, ^{28}Si, and ^{80}Br used here are 1.007 951, 27.976 929, and 79.904 000, respectively. Then, we artificially cool the entire system for 0.3 ps to reduce the temperature of the target to the initial temperature (i.e., 300 K). After the surface profile and etching characteristics become stable statistically [typically after 10 ML (720 particles) irradiation], the etching characteristics such as yields, stoichiometry, and surface structures are analyzed. All data shown here were obtained by averaging over more than 500 ion bombardments after a 10 ML impact.

In Fig. 4, Si etch yields by monoenergetic HBr^+ and Br^+ beams are shown as a function of ion energy (E_i). Si yields by Br^+ (Y_{Br^+}) exhibited a distinct power-law relationship, where $Y_{Br^+} \propto E_i^{0.40}$. This is close to the scaling of Steinbruchel,[18] $Y \propto \sqrt{E_i}$. In a previous experiment by Tachi *et al.*,[14] Y_{Br^+} exhibited an increasing power law trend up to 500 eV. Our simulation results qualitatively agreed with the results of this experiment. The difference between the yields by HBr^+ (Y_{HBr^+}) and Y_{Br+} was quite small in the high-energy region, i.e., $Y_{HBr^+}=Y_{Br^+}$ for $E_i>100$ eV. In contrast, $Y_{HBr^+}>Y_{Br^+}$ for $E_i<100$ eV.

The typical surface structures for HBr^+ and Br^+ with translational energies of 50 and 300 eV are shown in

TABLE I. Parameter set for Si/H/Br systems. The energy and length units are 50.0 kcal/mol (2.17 eV) and 2.0951 Å, respectively.

v_{HH} [a]	$A_{HH}=27.35$	h_{HHH} [b]	$\lambda_{HHH}=224.407$	h_{HHBr} [b]	$\lambda_{HHBr}=738.128$	h_{HSiH} [c]	$\lambda_{HSiH}=96.2240$
	$B_{HH}=0.07157$		$\gamma^{H}_{HHH}=C_{HH}$		$\gamma^{H}_{HHBr}=C_{HH}$		$\gamma^{H}_{HSiH}=C_{SiH}$
	$C_{HH}=1.711$		$a^{H}_{HHH}=a_{HH}$		$a^{H}_{HHBr}=a_{HH}$		$a^{H}_{HSiH}=a_{SiH}$
	$p_{HH}=1.627$				$\gamma^{Br}_{HHBr}=C_{HBr}$		$\theta^{0}_{HSiH}=110$
	$a_{HH}=1.2$	h_{SiHSi} [b]	$\lambda_{SiHSi}=211.693$		$a^{Br}_{HHBr}=a_{HBr}$		$\alpha_{HSiH}=1.29$
			$\gamma^{Si}_{SiHSi}=C_{SiH}$				
v_{SiH} [a]	$A_{SiH}=31.02$		$a^{Si}_{SiHSi}=a_{SiH}$	h_{HBrBr} [b]	$\lambda_{HBrBr}=368.386$	h_{HSiSi} [c]	$\lambda_{HSiSi}=39.3619$
	$B_{SiH}=0.2380$				$\gamma^{H}_{HBrBr}=C_{HBr}$		$\gamma^{H}_{HSiSi}=C_{SiH}$
	$C_{SiH}=2.520$	h_{HBrH} [b]	$\lambda_{HBrH}=2427.84$		$a^{H}_{HBrBr}=a_{HBr}$		$a^{H}_{HSiSi}=a_{SiH}$
	$p_{SiH}=2.213$		$\gamma^{H}_{HBrH}=C_{HBr}$		$\gamma^{Br}_{HBrBr}=C_{BrBr}$		$\gamma^{Si}_{HSiSi}=C_{SiSi}$
	$a_{SiH}=1.8$		$a^{H}_{HBrH}=a_{HBr}$		$a^{Br}_{HBrBr}=a_{BrBr}$		$a^{Si}_{HSiSi}=a_{SiSi}$
							$\theta^{0}_{HSiSi}=110$
v_{HBr} [a]	$A_{HBr}=89.96$	h_{BrHBr} [b]	$\lambda_{BrHBr}=2427.84$	h_{SiBrH} [b]	$\lambda_{SiBrH}=428.300$		$\alpha_{HSiSi}=1.3$
	$B_{HBr}=0.1756$		$\gamma^{Br}_{BrHBr}=C_{HBr}$		$\gamma^{Si}_{SiBrH}=C_{SiBr}$		
	$C_{HBr}=3.660$		$a^{Br}_{BrHBr}=a_{HBr}$		$a^{Si}_{SiBrH}=a_{SiBr}$	h_{HSiBr} [c]	$\lambda_{HSiBr}=89.5963$
	$p_{HBr}=2.488$				$\gamma^{H}_{SiBrH}=C_{HBr}$		$\gamma^{H}_{HSiBr}=C_{SiH}$
	$a_{HBr}=1.8$	h_{BrBrBr} [b]	$\lambda_{BrBrBr}=83.8451$		$a^{H}_{SiBrH}=a_{HBr}$		$a^{H}_{HSiBr}=a_{SiH}$
			$\gamma^{Br}_{BrBrBr}=C_{BrBr}$				$\gamma^{Br}_{HSiBr}=C_{SiBr}$
v_{BrBr} [a]	$A_{BrBr}=13.65$		$a^{Br}_{BrBrBr}=a_{BrBr}$	h_{SiHBr} [b]	$\lambda_{SiHBr}=837.168$		$a^{Br}_{HSiBr}=a_{SiBr}$
	$B_{BrBr}=0.7084$				$\gamma^{Si}_{SiHBr}=C_{SiH}$		$\theta^{0}_{HSiBr}=110$
	$C_{BrBr}=1.445$	h_{SiBrSi} [b]	$\lambda_{SiBrSi}=110.817$		$a^{Si}_{SiHBr}=a_{SiH}$		$\alpha_{BrSiSi}=1.29$
	$p_{BrBr}=4.649$		$\gamma^{Si}_{SiBrSi}=C_{SiBr}$		$\gamma^{Br}_{SiHBr}=C_{HBr}$		
	$a_{BrBr}=1.8$		$a^{Si}_{SiBrSi}=a_{SiBr}$		$a^{Br}_{SiHBr}=a_{HBr}$	h_{BrSiBr} [c]	$\lambda_{BrSiBr}=100.743$
							$\gamma^{Br}_{BrSiBr}=C_{SiBr}$
v_{SiBr} [a]	$A_{SiBr}=15.87$	h_{BrBrSi} [b]	$\lambda_{BrBrSi}=86.6502$	h_{HHSi} [b]	$\lambda_{HHSi}=254.519$		$a^{Br}_{BrSiBr}=a_{SiBr}$
	$B_{SiBr}=0.3938$		$\gamma^{Br}_{BrBrSi}=C_{BrBr}$		$\gamma^{H}_{HHSi}=C_{HH}$		$\theta^{0}_{BrSiBr}=105$
	$C_{SiBr}=2.749$		$a^{Br}_{BrBrSi}=a_{BrBr}$		$a^{H}_{HHSi}=a_{HH}$		$\alpha_{BrSiBr}=1.3$
	$p_{SiBr}=5.186$		$\gamma^{Si}_{BrBrSi}=C_{SiBr}$		$\gamma^{Si}_{HHSi}=C_{SiH}$		
	$a_{SiBr}=2.5$		$a^{Si}_{BrBrSi}=a_{SiBr}$		$a^{Si}_{HHSi}=a_{SiH}$	h_{BrSiSi} [c]	$\lambda_{BrSiSi}=19.0190$
							$\gamma^{Br}_{BrSiSi}=C_{SiBr}$
v_{SiSi} [a]	$A_{SiSi}=7.049556277$						$a^{Br}_{BrSiSi}=a_{SiBr}$
	$B_{SiSi}=0.602245584$						$\gamma^{Si}_{BrSiSi}=C_{SiSi}$
	$C_{SiSi}=1$						$a^{Si}_{BrSiSi}=a_{SiSi}$
	$p_{SiSi}=4$						$\theta^{0}_{BrSiSi}=110$
	$a_{SiSi}=1.8$						$\alpha_{BrSiSi}=1$
						h_{SiSiSi} [c]	$\lambda_{SiSiSi}=16.404$
							$\gamma^{Si}_{SiSiSi}=1.0473$
							$a^{Si}_{SiSiSi}=a_{SiSi}$
							$\theta^{0}_{SiSiSi}=109.4712206$
							$\alpha_{SiSiSi}=1$

[a]Equation (2).
[b]Equation (3).
[c]Equation (4).

Figs. 5 and 6, respectively. At the same ion energies, the Br coverage and the penetration depth of Br atoms were almost the same for HBr^+ and Br^+ (Figs. 5 and 6). As the ion energies increased, the Br coverage and the thickness of the reaction layer increased, while the H coverage was almost constant. H has approximately 1% of the translational energy of the cluster ions due to the HBr mass ratio (=1.0/79.9). Hence, H cannot penetrate into the lattice by its own translational energy and was just supplied on the top surface. After that, H was drawn into the reaction layer by the collisions caused by the following ion impacts. As a result, the thickness of the H distribution was almost the same as that of the Br distribution. As discussed here, H atoms in HBr^+ do not cause a dramatic difference in the reaction layers as compared to the cases of Br^+ impact. The degree of physical damages by the energetic bombardment is mainly determined by the contribution of Br^+. On the other hand, a typical surface during the monatomic H^+ irradiation (20 eV) is

TABLE II. Bond energies (potential minimums) and bond lengths calculated using our two-body functions.

	Bond energy (eV)	Bond length (Å)
H–H	4.83	0.775
Si–H	3.36	1.58
H–Br	4.03	1.44
Si–Si	2.17	2.35
Si–Br	3.67	2.32
Br–Br	2.06	2.34

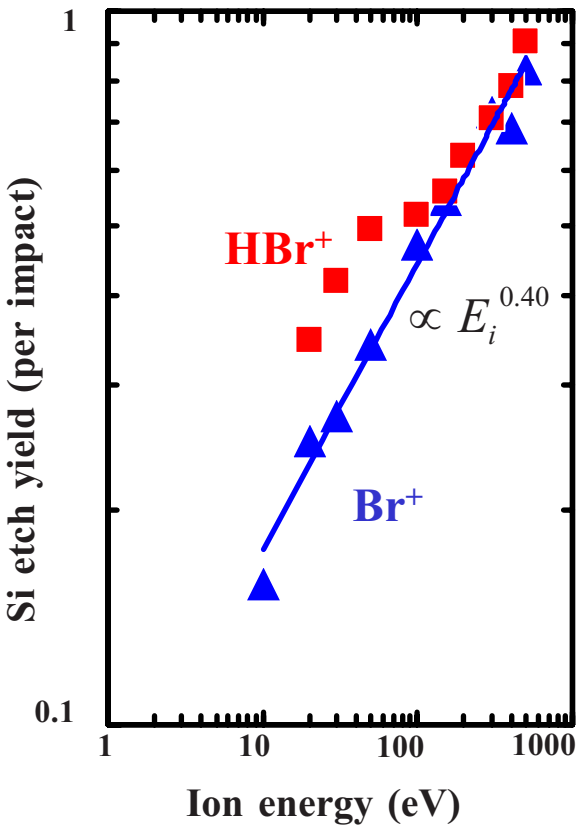

FIG. 4. (Color online) Si etch yield as a function of ion energy.

shown in Fig. 7, where we observed that H^+ could penetrate into the lattice to more than 30 nm because H^+ itself has a large translation energy. In this case, Si yield by H^+ was almost zero because the mass of H is very small and the momentum transfer from ^1H to ^{28}Si is extremely small.

Finally, the stoichiometry of Si etch yields was analyzed according to the bond number (the number of atoms binding with Si), as shown in Fig. 8. Products consisting of only H and Br are shown in Fig. 9. H atoms in HBr^+ behave like H radicals so that the etch yields by HBr^+ were chemically

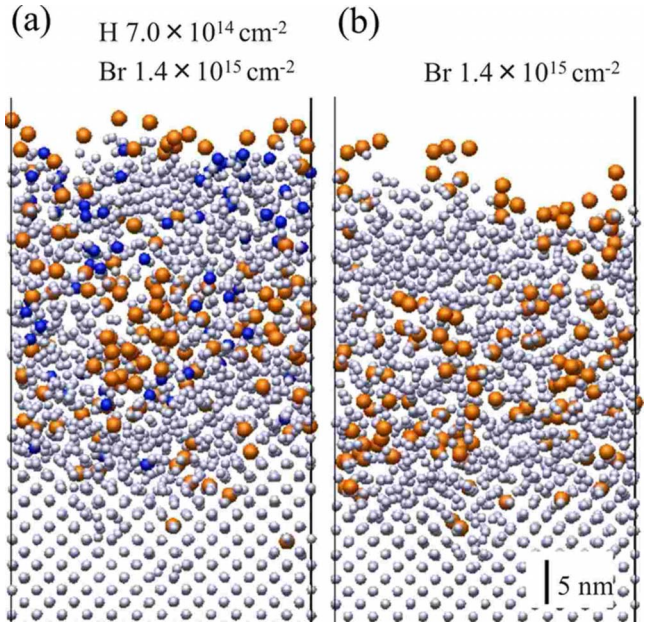

FIG. 6. (Color online) Typical surface structures for (a) HBr^+ and (b) Br^+ with a translational energy of 300 eV.

enhanced as compared to those by Br^+ due to the additional formation of Si–H bonds. Si products that included more than three bonds increased for HBr^+ as compared to Br^+, as shown in Fig. 9. About half of the H atoms were removed by forming Si–H bonds. The remaining atoms were directly reflected without getting absorbed by the surface atoms or sputtered by the subsequent energetic ion bombardment. In addition, H is likely to maintain its translation energy during collisions with surface Si atoms so that the probability to form Si–H bonds is relatively small.

On the other hand, the stoichiometries were almost the same for HBr^+ and Br^+ at 300 eV, as shown in Fig. 8. First, the Si etch products with less than two bonds were the dominant components. This indicates that the physical effect is more effective, i.e., the contribution of the chemical

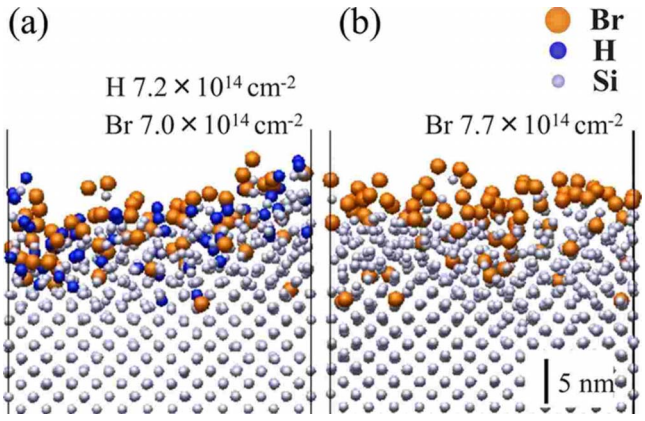

FIG. 5. (Color online) Typical surface structures for (a) HBr^+ and (b) Br^+ with a translational energy of 50 eV.

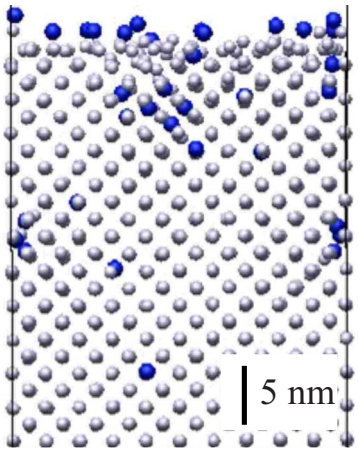

FIG. 7. (Color online) Typical surface structure for H^+ with a translational energy of 20 eV.

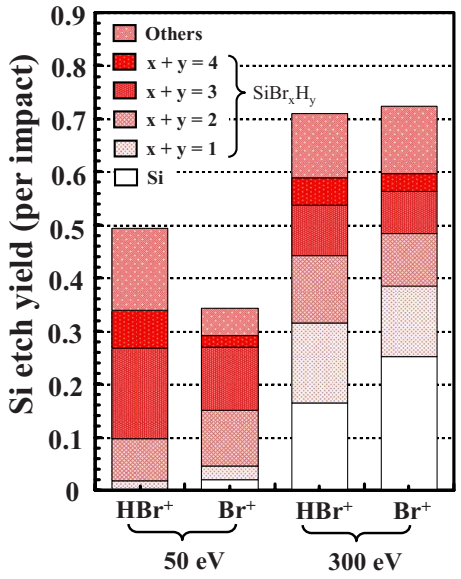

FIG. 8. (Color online) Stoichiometry of Si etch yield.

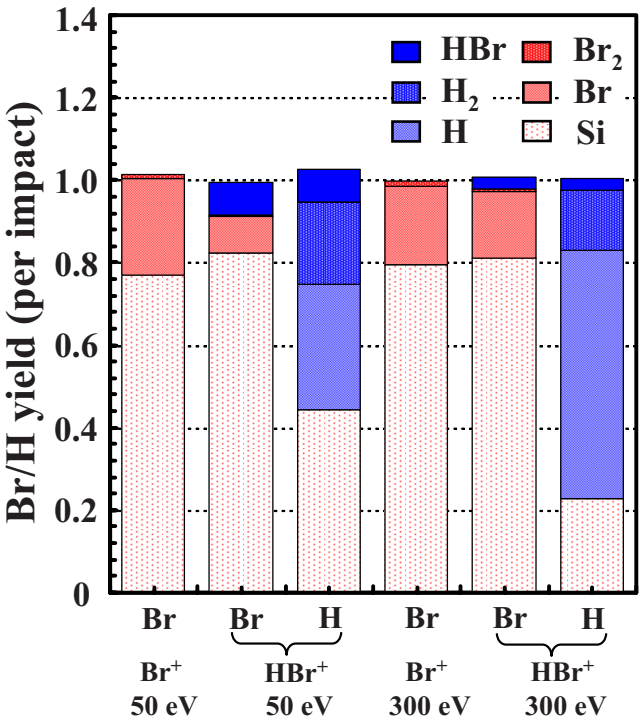

FIG. 9. (Color online) Stoichiometries of Br and H yield per ion impact. Note that the Br and H yields should be 1 to balance the influx and outflux.

enhancement by forming highly halogenated or hydrogenated products is less effective as compared to the cases of a 50 eV ion impact. Second, 75% of H was removed without Si–H bonds, as confirmed by Fig. 9. Therefore, $Y_{HBr^+}=Y_{Br^+}$ for $E_i>100$ eV.

IV. SUMMARY

In summary, we developed a new classical interatomic potential model for Si/H/Br systems based on the SW model. This potential model enables us to perform Si etching simulations by HBr^+-containing plasmas, which have been frequently used in state-of-the-art Si etching processes. Our simulation results revealed the difference between monoenergetic HBr^+ and Br^+ beams. In the high-energy region, Si etch yields by both HBr^+ and Br^+ were almost the same and obeyed a power-law relationship close to Steinbruchel's scaling. On the other hand, the Si yield by HBr^+ was enhanced by a large amount than that using this scaling due to the chemical enhancement by additional H atoms, where H in HBr^+ has a fairly small portion of the translational energy and behaves like a radical. At present, such discussion may be realized primarily in the numerical simulation and we believe advances in the MD technique for plasma processing technologies are imperative.

[1]International Technology Roadmap for Semiconductors (ITRS).
[2]For example, H. Ohta and S. Hamaguchi, J. Vac. Sci. Technol. A **19**, 2373 (2001).
[3]M. A. Leeberman and A. J. Lichtenberg, *Principles of Plasma Discharges and Materials Processing*, 2nd ed. (Wiley, Hoboken, NJ, 2005).
[4]H. Abe, M. Yoneda, and N. Fujiwara, Jpn. J. Appl. Phys. **47**, 1435 (2008).
[5]A. Iwakawa, T. Nagaoka, H. Ohta, K. Eriguchi, and K. Ono, Jpn. J. Appl. Phys. **47**, 8560 (2008).
[6]F. H. Stillinger and T. A. Weber, Phys. Rev. B **31**, 5262 (1985); J. Chem. Phys. **88**, 5123 (1988); Phys. Rev. Lett. **62**, 2144 (1989).
[7]H. Feil, J. Dieleman, and B. J. Garrison, J. Appl. Phys. **74**, 1303 (1993).
[8]H. Ohta and S. Hamaguchi, J. Chem. Phys. **115**, 6679 (2001).
[9]V. V. Smirnov, A. V. Stengach, K. G. Gaynullin, V. A. Pavlovsky, S. Rauf, P. J. Stout, and P. L. G. Ventzek, J. Appl. Phys. **97**, 093302 (2005).
[10]V. V. Smirnov, A. V. Stengach, K. G. Gaynullin, V. A. Pavlovsky, S. Rauf, and P. L. G. Ventzek, J. Appl. Phys. **101**, 053307 (2007).
[11]H. Ohta, A. Iwakawa, K. Eriguchi, and K. Ono, J. Appl. Phys. **104**, 073302 (2008).
[12]A. Iwakawa, H. Ohta, K. Eriguchi, and K. Ono, Jpn. J. Appl. Phys. **47**, 6464 (2008).
[13]H. Ohta, T. Nagaoka, K. Eriguchi, and K. Ono, Jpn. J. Appl. Phys. (to be published).
[14]S. Tachi and S. Okudaira, J. Vac. Sci. Technol. B **4**, 459 (1986).
[15]S. A. Vitale, H. Chae, and H. H. Sawin, J. Vac. Sci. Technol. A **19**, 2197 (2001).
[16]D. E. Hanson, A. F. Voter, and J. D. Kress, J. Chem. Phys. **110**, 5983 (1999).
[17]M. J. Frisch, G. W. Trucks, H. B. Schlegel *et al.*, *Gaussian 03* (Gaussian, Inc., Pittsburgh, PA, 2003).
[18]C. Steinbruchel, Appl. Phys. Lett. **55**, 1960 (1989).